Mott physics and spin fluctuations: A unified framework

Thomas Ayral[1,2,*] and Olivier Parcollet[2]
[1]*Centre de Physique Théorique, Ecole Polytechnique, CNRS-UMR 7644, 91128 Palaiseau, France*
[2]*Institut de Physique Théorique (IPhT), CEA, CNRS, UMR CNRS 3681, 91191 Gif-sur-Yvette, France*
(Received 30 March 2015; published 3 September 2015)

We present a formalism for strongly correlated electron systems which consists in a local approximation of the dynamical three-leg interaction vertex. This vertex is self-consistently computed using a quantum impurity model with dynamical interactions in the charge and spin channels, similar to dynamical mean field theory approaches. The electronic self-energy and the polarization are both frequency and momentum dependent. The method interpolates between the spin-fluctuation or *GW* approximations at weak coupling and the atomic limit at strong coupling. We apply the formalism to the Hubbard model on a two-dimensional square lattice and show that as interactions are increased towards the Mott insulating state, the local vertex acquires a strong frequency dependence, driving the system to a Mott transition, while at low enough temperatures the momentum dependence of the self-energy is enhanced due to large spin fluctuations. Upon doping, we find a Fermi arc in the one-particle spectral function, which is one signature of the pseudogap state.

DOI: 10.1103/PhysRevB.92.115109 PACS number(s): 71.10.Fd, 71.27.+a, 71.30.+h

Strongly correlated electronic systems such as high-temperature cuprate superconductors are a major challenge in condensed-matter physics. One theoretical approach to cuprates emphasizes the effect of long-range bosonic fluctuations on the electronic fluid, for example, long-range antiferromagnetic (AF) fluctuations due to a quantum critical point [1–6]. These bosonic fluctuations are also central to approaches such as the two-particle self-consistent approximation (TPSC [7–11]), the *GW* approximation [12], and the fluctuation-exchange approximation (FLEX [13]).

Another approach focuses, following Anderson [14], on describing the Mott transition and the doped Mott insulator. In recent years, dynamical mean field theory (DMFT) [15] and its cluster extensions such as cellular DMFT (CDMFT) [16,17] or the dynamical cluster approximation (DCA) [18–20] have allowed for tremendous theoretical progress on the Mott transition both for models and realistic computations of strongly correlated materials [21]. In particular, numerous works have been devoted to the one-band Hubbard model, mapping out its phase diagram, studying the d-wave superconducting order and the pseudogap [22–45]. Cluster DMFT is one of the few methods designed for the strong-interaction regime to have a simple control parameter, namely, the size N_c of the cluster or the momentum resolution of the electronic self-energy. It interpolates between the DMFT solution ($N_c = 1$) and the exact solution of the Hubbard model ($N_c = \infty$). Despite its success, this method nonetheless suffers from severe limitations: (i) It does not include the effect of long-range bosonic modes of wavelengths larger than the cluster size; (ii) the negative sign problem of continuous-time quantum Monte Carlo has so far precluded the convergence of the cluster solutions with respect to N_c in the most important regimes, such as the pseudogap; and (iii) the **k** resolution of the self-energy is still quite coarse in DCA (typically eight or 16 patches in the Brillouin zone—see, e.g., Refs. [31,33,45,46]), or it relies on uncontrolled *a posteriori* "periodization" techniques in CDMFT [17].

Several directions beyond cluster DMFT methods are currently under investigation to address these issues, such as *GW*+DMFT [47–53], the combination of DMFT with functional renormalization group methods [54], the dynamical vertex approximation (DΓA) [55–58], and the dual fermion (DF) or boson methods [59–61]. DΓA and DF require the manipulation of four-leg vertices and, in their ladder version, require the summation of selected classes of ladder diagrams. Simpler yet controlled methods are needed: Except for one-dimensional chains [62], neither DΓA nor DF has been applied to multiorbital systems to date.

In this Rapid Communication, we discuss a simple formalism that unifies the two points of view mentioned above while remaining comparatively lightweight. It is designed to encompass both Mott physics in the manner of DMFT and the effect of medium- and long-range bosonic modes. It interpolates between the atomic and the "fluctuation-exchange" limits upon going from strong to weak interactions. It consists in decoupling the electron-electron interaction by Hubbard-Stratonovich bosonic fields and making a local and self-consistent approximation of the lattice's electron-boson one-particle irreducible three-leg vertex, using a quantum impurity model similar to the one used in DMFT. Since this method approximates three-leg objects with a local expansion, we will call it TRILEX. Already at the single-site level, it produces, in some parameter regimes, a momentum-dependent self-energy and polarization, at a small computational cost, similar to solving extended DMFT (EDMFT) [63–65]. In the following, we introduce the method and then present the solution of its single-site version for the two-dimensional Hubbard model.

We focus on the Hubbard model defined by the following Hamiltonian:

$$H = \sum_{ij,\sigma} t_{ij} c^\dagger_{i\sigma} c_{j\sigma} + U \sum_i n_{i\uparrow} n_{i\downarrow}. \tag{1}$$

The indices i, j denote lattice sites, $\sigma = \uparrow, \downarrow$, $c^\dagger_{i\sigma}$ ($c_{i\sigma}$) is a fermionic creation (annihilation) operator, and $n_{i\sigma} \equiv c^\dagger_{i\sigma} c_{i\sigma}$. t_{ij} is the tight-binding hopping matrix [$t_{ij} = t(t')$ for (next-)

*thomas.ayral@polytechnique.edu

 ©2015 American Physical Society

nearest neighbors], while U is the on-site Coulomb interaction. We rewrite the operators of the interaction term as

$$U n_{i\uparrow} n_{i\downarrow} = \frac{1}{2} \sum_I U^I n_i^I n_i^I, \tag{2}$$

where U^I is the bare interaction in channel I, and $n_i^I \equiv \sum_{\sigma\sigma'} c_{i\sigma}^* \sigma^I_{\sigma\sigma'} c_{i\sigma'}$, where $\sigma^0 = \mathbf{1}$ and $\sigma^{x,y,z}$ are the Pauli matrices. Here, we consider one possible decoupling[1] which preserves the rotation symmetry of the action: The index I runs on $0,x,y,z$, $U^x = U^y = U^z \equiv U^{\rm sp}$, and $U^0 \equiv U^{\rm ch}$, and $U^{\rm sp}$ and $U^{\rm ch}$ satisfy $U = U^{\rm ch} - 3U^{\rm sp}$. We have two channels, denoted as $\eta = {\rm ch}, {\rm sp}$. We fix the ratio to $U^{\rm ch} = U/2$ and $U^{\rm sp} = -U/6$.[2] We now decouple (2) using real bosonic Hubbard-Stratonovich fields $\phi_i^I(\tau)$ in each channel and at each lattice site, so that the action now describes a lattice problem with a local electron-boson coupling:

$$S_{\rm latt} = \int_0^\beta d\tau \sum_{ij} c^*_{i\sigma\tau} \{\partial_\tau + t_{ij}\} c_{j\sigma\tau} + \sum_{i,I} \left[\frac{1}{2} (-U^I)^{-1} \phi^I_{i\tau} \phi^I_{i\tau} + \lambda^I \phi^I_{i\tau} n^I_{i\tau} \right]. \tag{3}$$

$c^*_{i\sigma\tau}$ and $c_{i\sigma\tau}$ are conjugate β-antiperiodic Grassmann fields, and $\lambda^I = 1$. The lattice Green's functions $G(\mathbf{k},i\omega)$ and $W^\eta(\mathbf{q},i\Omega)$ (the Fourier transforms of $-\langle c_{i\sigma\tau} c^*_{j\sigma 0}\rangle$ and $-\langle \phi^\eta_{i\sigma\tau} \phi^\eta_{j\sigma 0}\rangle$, respectively) are given by Dyson equations,

$$G(\mathbf{k},i\omega) = [i\omega + \mu - \varepsilon(\mathbf{k}) - \Sigma(\mathbf{k},i\omega)]^{-1}, \tag{4a}$$

$$W^\eta(\mathbf{q},i\Omega) = U^\eta [1 - U^\eta P^\eta(\mathbf{q},i\Omega)]^{-1}. \tag{4b}$$

$\mathbf{k}$ and $\mathbf{q}$ are momentum variables, $i\omega$ ($i\Omega$) stands for a fermionic (bosonic) Matsubara frequency, $\varepsilon(\mathbf{k})$ is the Fourier transform of t_{ij}, and μ is the chemical potential. The fermionic and bosonic self-energies Σ and P^η are given by the exact expressions (in the paramagnetic, normal phase) (see, e.g., Ref. [67])

$$\Sigma(\mathbf{k},i\omega) = -\sum_{\substack{\mathbf{q},i\Omega,\\ \eta={\rm ch,sp}}} m_\eta \lambda^\eta G_{\substack{\mathbf{q}+\mathbf{k},\\ i\omega+i\Omega}} W^\eta_{\mathbf{q},i\Omega} \Lambda^\eta_{\substack{\mathbf{k},\mathbf{q},\\ i\omega,i\Omega}}, \tag{5a}$$

$$P^\eta(\mathbf{q},i\Omega) = 2\sum_{\mathbf{k},i\omega} \lambda^\eta G_{\substack{\mathbf{q}+\mathbf{k},\\ i\omega+i\Omega}} G_{\mathbf{k},i\omega} \Lambda^\eta_{\substack{\mathbf{k},\mathbf{q},\\ i\omega,i\Omega}}. \tag{5b}$$

Here, $m_{\rm ch} = 1$ and $m_{\rm sp} = 3$. $\Lambda^\eta(\mathbf{k},\mathbf{q},i\omega,i\Omega)$ is the exact one-particle irreducible electron-boson coupling (or Hedin) vertex, namely, the effective interaction between electrons and bosons renormalized by electronic interactions.

The main point of this Rapid Communication consists in approximating the vertex $\Lambda^\eta(\mathbf{k},\mathbf{q},i\omega,i\Omega)$ by the local, but two-frequency-dependent, $\Lambda^\eta_{\rm imp}(i\omega,i\Omega)$ computed from a self-consistent quantum impurity problem:

$$\Lambda^\eta(\mathbf{k},\mathbf{q},i\omega,i\Omega) \approx \Lambda^\eta_{\rm imp}(i\omega,i\Omega). \tag{6}$$

This strategy differs radically from DMFT, EDMFT, and GW+DMFT which approximate the self-energy Σ (and P), and DΓA, which approximates four-leg vertices, not Λ. It implies that our Σ and P [computed from Eqs. (5a) and (5b)] are, in some parameter regimes, strongly *momentum dependent* while containing *local* vertex corrections essential to capture the Mott physics [50].

The action of the impurity model reads

$$S_{\rm imp} = -\iint_0^\beta d\tau d\tau' \sum_\sigma c^*_{\sigma\tau} \mathcal{G}^{-1}(\tau - \tau') c_{\sigma\tau'} + \frac{1}{2} \sum_{I=0,x,y,z} \iint_0^\beta d\tau d\tau' n^I_\tau \mathcal{U}^I(\tau - \tau') n^I_{\tau'}. \tag{7}$$

This is an Anderson impurity with retarded charge-charge ($I = 0$) and spin-spin ($I = x,y,z$) interactions. The bosonic fields ϕ^I have been integrated out to obtain a fermionic action with retarded interactions amenable to numerical computations. We compute the fermionic three-point correlation functions to reconstruct the electron-boson vertex $\Lambda^\eta_{\rm imp}$ (as shown in Supplemental Material B [66]). Finally, $\mathcal{G}$ and $\mathcal{U}^\eta$ derive from the self-consistency conditions as follows,

$$\mathcal{G}^{-1}(i\omega) = G^{-1}_{\rm loc}(i\omega) + \Sigma_{\rm loc}(i\omega), \tag{8a}$$

$$[\mathcal{U}^\eta]^{-1}(i\Omega) = \left[W^\eta_{\rm loc}\right]^{-1}(i\Omega) + P^\eta_{\rm loc}(i\Omega), \tag{8b}$$

where, for any X, $X_{\rm loc}(i\omega) \equiv \sum_{\mathbf{k}} X(\mathbf{k},i\omega)$. At convergence, this ensures that $G_{\rm loc} = G_{\rm imp}$ and $W^\eta_{\rm loc} = W^\eta_{\rm imp}$. W^η and the susceptibility χ^η are related by

$$W^\eta(\mathbf{q},i\Omega) = U^\eta - U^\eta \chi^\eta(\mathbf{q},i\Omega) U^\eta. \tag{9}$$

The computational scheme is illustrated in Fig. 1. From $\Lambda^\eta_{\rm imp}(i\omega,i\Omega)$, we compute $\Sigma(\mathbf{k},i\omega)$ and $P^\eta(\mathbf{q},i\Omega)$, which are then used to compute $\mathcal{G}$ and $\mathcal{U}^\eta$ for (7). We solve Eq. (7) exactly by a continuous-time quantum Monte Carlo algorithm [69] in the hybridization expansion [70] with retarded density-density [71] and vector spin-spin interactions [72]. The computation of the three-point functions is implemented following Ref. [73]. We iterate until convergence is reached. Our implementation is based on the TRIQS library [74]. Equation (7) could also be solved by an interaction-expansion solver.

This construction makes TRILEX exact in two limits: (i) At small interaction strengths, the local vertex reduces to the bare, frequency-independent vertex λ^η so that Σ is given by one-loop diagrams, as in spin-fluctuation theory in its simplest form (spin channel only), the GW approximation (charge channel only), or in FLEX limited to particle-hole diagrams; similarly, P^η turns into the "bubble" diagram; (ii) in the atomic limit ($t = 0$), the effective local action turns into an atomic problem, $\Lambda^\eta_{\rm imp}$ into the atomic vertex $\Lambda^\eta_{\rm at}$ [Eq. (A1)], and Σ and P^η become local, atomic self-energies.

Let us now apply the TRILEX method to the Hubbard model on a square lattice. All energies are given in units of

[1] Other decouplings are possible, for instance, index I can run only on $0,z$ (charge and longitudinal spin channel only). In this case, $U^{\rm ch}$ and $U^{\rm sp}$ obey the relation $U = U^{\rm ch} - U^{\rm sp}$. This decoupling breaks the rotation symmetry of the action.

[2] The influence of this choice is investigated in Supplemental Material D [66].

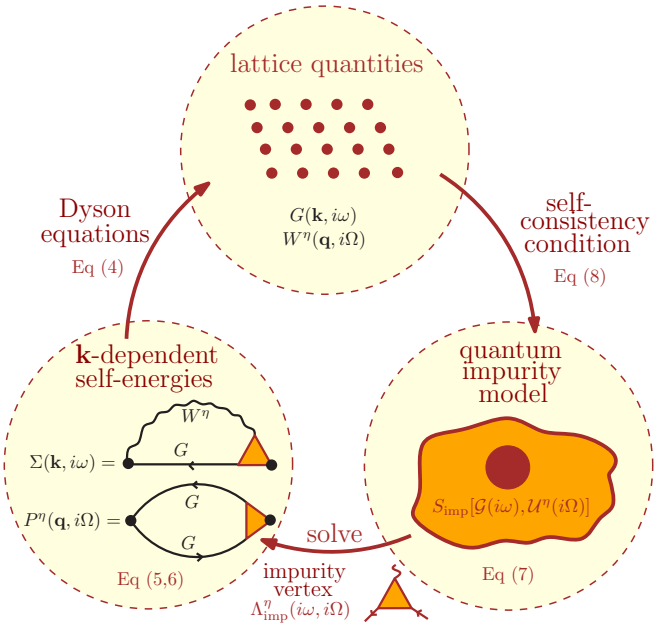

FIG. 1. (Color online) The TRILEX self-consistency loop.

the half bandwidth $D = 4|t|$. The Brillouin zone is discretized on a 64×64 momentum mesh.[3] We restrict ourselves to the paramagnetic normal phase.

[3]We have checked that the 64×64 discretization yields the same results as the 32×32 discretization.

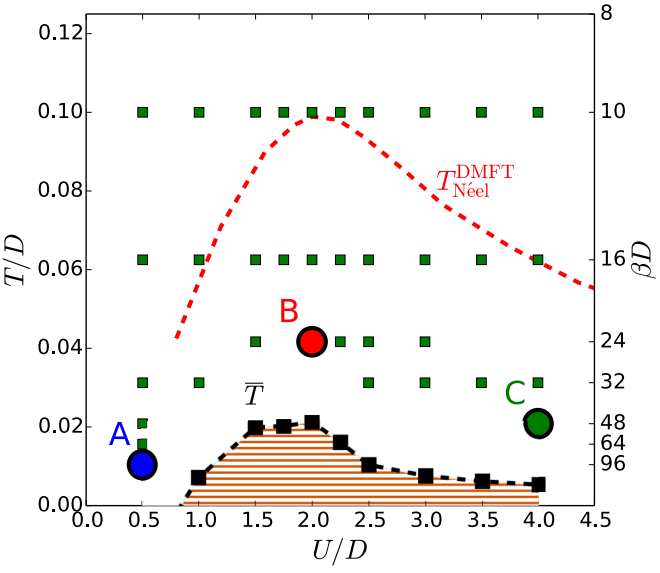

FIG. 2. (Color online) (T,U) phase diagram (half filling, $t' = 0$). The green squares denote converged TRILEX solutions. A, B, and C are defined as (A) $\beta D = 96$, $U/D = 0.5$, (B) $\beta D = 24$, $U/D = 2$, and (C) $\beta D = 48$, $U/D = 4$. The red dotted line denotes $T^{\rm DMFT}_{\rm Néel}$ for the square lattice (from Ref. [68]). The black squares denote $\overline{T}$ (temperature below which one cannot obtain stable solutions, hatched region); the black dashed line is a guide to the eye.

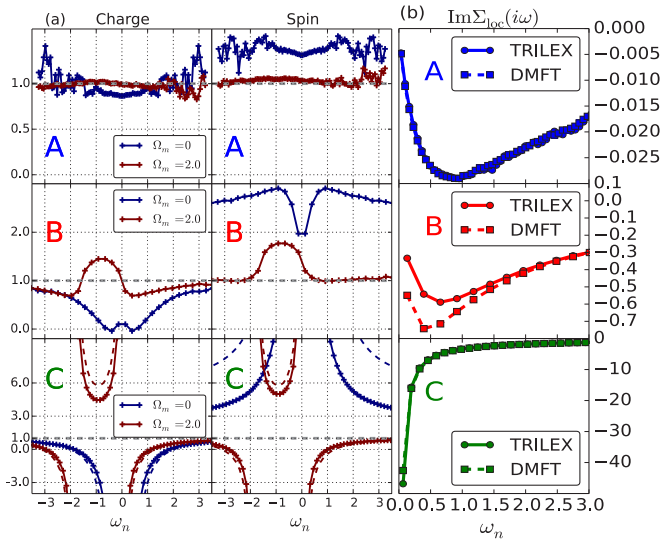

FIG. 3. (Color online) Left: Evolution of the local vertex $\mathrm{Re}\,\Lambda^\eta_{\rm imp}(i\omega_n,i\Omega_m)$ as a function of ω_n (half filling, $t' = 0$). A, B, and C are defined in Fig. 2. The dashed lines denote the atomic vertex $\Lambda^\eta_{\rm at}$ [Eq. (A1)]. Right: $\mathrm{Im}\,\Sigma_{\rm loc}(i\omega_n)$ for TRILEX and DMFT (paramagnetic phase).

In Fig. 2, we present the phase diagram in the (T,U) plane at half filling. We obtain converged solutions until a temperature $\overline{T}$ (see below). The evolution of the local vertex and self-energy (respectively lattice self-energy and polarizations) is presented in Fig. 3 (respectively Fig. 4) for the points A, B, and C of Fig. 2. At weak coupling (point A), the local vertex $\Lambda^\eta_{\rm imp}(i\omega,i\Omega)$ reduces to the bare vertex $\lambda = 1$ at large frequencies, up to numerical noise [Fig. 3(a), upper panels]. The spin polarization

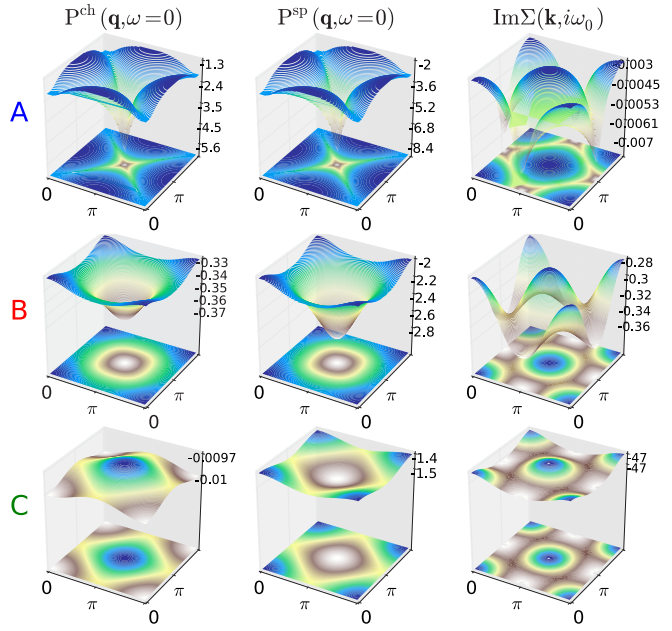

FIG. 4. (Color online) Momentum dependence of the self-energy and polarization (half filling, $t' = 0$). A, B, and C are defined in Fig. 2. Left: $\mathrm{Re}\,P^{\rm ch}(\mathbf{q},\omega = 0)$. Middle: $\mathrm{Re}\,P^{\rm sp}(\mathbf{q},\omega = 0)$. Right: $\mathrm{Im}\,\Sigma(\mathbf{k},i\omega_0)$.

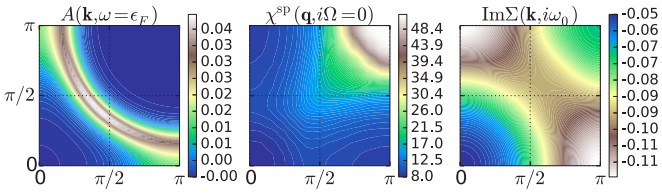

FIG. 5. (Color online) From left to right: $A(\mathbf{k},\omega=0)$, $\chi(\mathbf{q},i\Omega=0)$, and $\mathrm{Im}\,\Sigma(\mathbf{k},i\omega_0)$ in the doped case: $U/D=1.8$, $t'=-0.4t$, $\beta D=96$, $\delta=10\%$.

[hence the spin susceptibility—see Eq. (9)] becomes sharply peaked at the AF wave vector $\mathbf{Q}=(\pi,\pi)$ (Fig. 4, upper panels), reflecting the nesting features of the Fermi surface. As a result, the self-energy acquires a strong $\mathbf{k}$ dependence at $(\pi,0)$ (Fig. 4), but its local part is the same as the DMFT self-energy [Fig. 3(b)]. At strong coupling (point C), the vertex becomes similar to the atomic vertex [Fig. 3(a), lower panels]. Furthermore, the self-energy and polarization are weakly momentum dependent (Fig. 4, lower panels), in agreement with cluster DMFT calculations; the self-energy of TRILEX is very close to the DMFT self-energy [Fig. 3(b)]. Finally, at intermediate coupling (point B), $\Lambda^{\eta}_{\mathrm{imp}}(i\omega,i\Omega)$ acquires frequency structures which interpolate between A and C [Fig. 3(a), middle panels], while Σ is strongly momentum dependent and its local part departs from the DMFT self-energy [Fig. 3(b), middle panels]. Interestingly, the TRILEX self-energy is more coherent than the DMFT self-energy, contrary to the trend observed in cluster DMFT [75]. This may be due to the absence of short-range singlet physics in TRILEX which may be investigated using a small cluster extension.

Contrary to DMFT, the convergence of metastable paramagnetic solutions below a long-range ordering temperature is not possible, since the susceptibilities are not by-products of the calculation, but directly feed back into the self-consistency loop through W^{η} [see Eq. (9)]. We obtain stable paramagnetic solutions at much lower temperatures compared to the Néel temperature computed in DMFT [68] until $\overline{T}$, as a result of nonlocal fluctuations beyond DMFT. The temperature $\overline{T}$ is determined by extrapolating the inverse static AF susceptibility (see Fig. A1 in the Supplemental Material [66]). Below and in the vicinity of $\overline{T}$, we obtain unstable solutions because of very small denominators in W^{sp}. Whether we have, within our approximate scheme, finite but very large correlation lengths (as seen, e.g., in Ref. [57]) or an actual AF transition (thus violating the Mermin-Wagner theorem), is left for future studies.

Let us now turn to the effect of doping. In Fig. 5, we present results for $t'=-0.4t$, $\beta D=96$, and an intermediate interaction strength ($U=1.8$, close to point B). The spectral function displays Fermi arcs (Fig. 5, left panel), as observed in experiments [76] and in cluster DMFT [35,37,38,42–44,77]. Let us emphasize that this is obtained by solving a *single-site* quantum impurity problem, a far easier task than solving cluster impurities. The Fermi arc is a consequence of the large static spin susceptibility at the AF wave vector (Fig. 5, middle panel), which translates into a large imaginary part of the self-energy (Fig. 5, right panel). The corresponding variation of the spectral weight on the Fermi surface is rather mild compared to the experimental results due to the moderate correlation length ($\xi_{\mathrm{AF}}\sim 2$ unit spacings) for these parameters. This variation is also smaller than cluster DMFT results, which may indicate that improving the description of short-range correlations will yield closer agreement to experiments.

Finally, we examine the influence of the ratio between the interaction in the charge and the spin channel. We observe that it does not impact either the fact that one can obtain stable solutions much below the DMFT Néel temperature ($\overline{T}$ mildly depends on the ratio), or the fulfillment of sum rules on the charge and spin susceptibility (see Supplemental Material D [66]). We have also tried alternative self-consistency conditions, e.g., $\chi^{\eta}_{\mathrm{loc}}=\chi^{\eta}_{\mathrm{imp}}$ instead of $W^{\eta}_{\mathrm{loc}}=W^{\eta}_{\mathrm{imp}}$. This, however, leads to a positive $\mathcal{U}^{\mathrm{sp}}(\tau)$ and hence to a severe sign problem in the quantum Monte Carlo at low temperatures.

In conclusion, we have presented the TRILEX formalism, which encompasses long-range spin-fluctuation effects and Mott physics. Because the competition between spin fluctuations and Mott physics can be described already at the single-site level, this computationally lightweight method may be a good starting point for studying correlated multiorbital systems where spin fluctuations play an important role, such as pnictide superconductors. Future investigations will include the extension to cluster schemes that interpolate between the single-site approximation and the exact solution of the model. With this extension, TRILEX will capture both long-range and short-range fluctuations. Moreover, the convergence of the method with cluster size may depend on the decoupling channel and, when done in the physically relevant channel, may be faster than cluster DMFT methods.

We acknowledge useful discussions with S. Andergassen, S. Biermann, M. Ferrero, A. Georges, D. Manske, G. Misguich, J. Otsuki, and A. Toschi. We thank H. Hafermann for help with implementing the measurement of the three-point correlation function. This work is supported by the FP7/ERC, under Grant Agreement No. 278472-MottMetals. Part of this work was performed using HPC resources from GENCI-TGCC (Grant No. 2015-t2015056112).

[1] A. V. Chubukov, D. Pines, and J. Schmalian, in *The Physics of Conventional and Unconventional Superconductors*, edited by K. H. Bennemann and J. B. Ketterson (Springer, Berlin, 2002), Chap. 22, p. 1349.
[2] K. B. Efetov, H. Meier, and C. Pépin, Nat. Phys. **9**, 442 (2013).
[3] Y. Wang and A. Chubukov, Phys. Rev. B **90**, 035149 (2014).
[4] M. A. Metlitski and S. Sachdev, Phys. Rev. B **82**, 075128 (2010).
[5] F. Onufrieva and P. Pfeuty, Phys. Rev. Lett. **102**, 207003 (2009).
[6] F. Onufrieva and P. Pfeuty, Phys. Rev. Lett. **109**, 257001 (2012).

[7] Y. M. Vilk, L. Chen, and A.-M. S. Tremblay, Phys. Rev. B **49**, 13267(R) (1994).

[8] A.-M. Daré, Y. M. Vilk, and A.-M. S. Tremblay, Phys. Rev. B **53**, 14236 (1996).

[9] Y. M. Vilk and A.-M. S. Tremblay, Europhys. Lett. **33**, 159 (1996).

[10] Y. Vilk and A.-M. S. Tremblay, J. Phys. I **7**, 1309 (1997).

[11] A.-M. S. Tremblay, in *Theoretical Methods for Strongly Correlated Systems*, edited by A. Avella and F. Mancini, Springer Series in Solid-State Sciences Vol. 171 (Springer, Berlin, 2011), pp. 409–453.

[12] L. Hedin, Phys. Rev. **139**, A796 (1965).

[13] N. Bickers and D. Scalapino, Ann. Phys. **193**, 206 (1989).

[14] P. W. Anderson, Science **235**, 1196 (1987).

[15] A. Georges, G. Kotliar, W. Krauth, and M. J. Rozenberg, Rev. Mod. Phys. **68**, 13 (1996).

[16] A. I. Lichtenstein and M. I. Katsnelson, Phys. Rev. B **62**, R9283 (2000).

[17] G. Kotliar, S. Y. Savrasov, G. Pálsson, and G. Biroli, Phys. Rev. Lett. **87**, 186401 (2001).

[18] M. H. Hettler, A. N. Tahvildar-Zadeh, M. Jarrell, T. Pruschke, and H. R. Krishnamurthy, Phys. Rev. B **58**, R7475 (1998).

[19] M. H. Hettler, M. Mukherjee, M. Jarrell, and H. R. Krishnamurthy, Phys. Rev. B **61**, 12739 (2000).

[20] T. A. Maier, M. Jarrell, T. Pruschke, and M. H. Hettler, Rev. Mod. Phys. **77**, 1027 (2005).

[21] G. Kotliar, S. Y. Savrasov, K. Haule, V. S. Oudovenko, O. Parcollet, and C. A. Marianetti, Rev. Mod. Phys. **78**, 865 (2006).

[22] B. Kyung, D. Sénéchal, and A.-M. S. Tremblay, Phys. Rev. B **80**, 205109 (2009).

[23] G. Sordi, P. Sémon, K. Haule, and A.-M. S. Tremblay, Phys. Rev. Lett. **108**, 216401 (2012).

[24] M. Civelli, M. Capone, A. Georges, K. Haule, O. Parcollet, T. D. Stanescu, and G. Kotliar, Phys. Rev. Lett. **100**, 046402 (2008).

[25] M. Ferrero, O. Parcollet, A. Georges, G. Kotliar, and D. N. Basov, Phys. Rev. B **82**, 054502 (2010).

[26] E. Gull, O. Parcollet, and A. J. Millis, Phys. Rev. Lett. **110**, 216405 (2013).

[27] A. Macridin, M. Jarrell, and Th. Maier, Phys. Rev. B **70**, 113105 (2004).

[28] T. A. Maier, M. Jarrell, A. Macridin, and C. Slezak, Phys. Rev. Lett. **92**, 027005 (2004).

[29] T. A. Maier, M. Jarrell, T. C. Schulthess, P. R. C. Kent, and J. B. White, Phys. Rev. Lett. **95**, 237001 (2005).

[30] T. A. Maier, M. S. Jarrell, and D. J. Scalapino, Phys. Rev. Lett. **96**, 047005 (2006).

[31] E. Gull, M. Ferrero, O. Parcollet, A. Georges, and A. J. Millis, Phys. Rev. B **82**, 155101 (2010).

[32] S. X. Yang, H. Fotso, S. Q. Su, D. Galanakis, E. Khatami, J. H. She, J. Moreno, J. Zaanen, and M. Jarrell, Phys. Rev. Lett. **106**, 047004 (2011).

[33] A. Macridin and M. Jarrell, Phys. Rev. B **78**, 241101(R) (2008).

[34] A. Macridin, M. Jarrell, T. A. Maier, P. R. C. Kent, and E. D'Azevedo, Phys. Rev. Lett. **97**, 036401 (2006).

[35] M. Jarrell, T. A. Maier, C. Huscroft, and S. Moukouri, Phys. Rev. B **64**, 195130 (2001).

[36] D. Bergeron, V. Hankevych, B. Kyung, and A.-M. S. Tremblay, Phys. Rev. B **84**, 085128 (2011).

[37] B. Kyung, V. Hankevych, A.-M. Daré, and A.-M. S. Tremblay, Phys. Rev. Lett. **93**, 147004 (2004).

[38] B. Kyung, S. S. Kancharla, D. Sénéchal, A.-M. S. Tremblay, M. Civelli, and G. Kotliar, Phys. Rev. B **73**, 165114 (2006).

[39] S. Okamoto, D. Sénéchal, M. Civelli, and A.-M. S. Tremblay, Phys. Rev. B **82**, 180511 (2010).

[40] G. Sordi, K. Haule, and A.-M. S. Tremblay, Phys. Rev. Lett. **104**, 226402 (2010).

[41] G. Sordi, P. Sémon, K. Haule, and A.-M. S. Tremblay, Sci. Rep. **2**, 547 (2012).

[42] M. Civelli, M. Capone, S. S. Kancharla, O. Parcollet, and G. Kotliar, Phys. Rev. Lett. **95**, 106402 (2005).

[43] M. Ferrero, P. S. Cornaglia, L. De Leo, O. Parcollet, G. Kotliar, and A. Georges, Europhys. Lett. **85**, 57009 (2009).

[44] M. Ferrero, P. S. Cornaglia, L. De Leo, O. Parcollet, G. Kotliar, and A. Georges, Phys. Rev. B **80**, 064501 (2009).

[45] E. Gull, O. Parcollet, P. Werner, and A. J. Millis, Phys. Rev. B **80**, 245102 (2009).

[46] N. S. Vidhyadhiraja, A. Macridin, C. Sen, M. Jarrell, and M. Ma, Phys. Rev. Lett. **102**, 206407 (2009).

[47] P. Sun and G. Kotliar, Phys. Rev. B **66**, 085120 (2002).

[48] P. Sun and G. Kotliar, Phys. Rev. Lett. **92**, 196402 (2004).

[49] S. Biermann, F. Aryasetiawan, and A. Georges, Phys. Rev. Lett. **90**, 086402 (2003).

[50] T. Ayral, P. Werner, and S. Biermann, Phys. Rev. Lett. **109**, 226401 (2012).

[51] T. Ayral, S. Biermann, and P. Werner, Phys. Rev. B **87**, 125149 (2013).

[52] P. Hansmann, T. Ayral, L. Vaugier, P. Werner, and S. Biermann, Phys. Rev. Lett. **110**, 166401 (2013).

[53] L. Huang, T. Ayral, S. Biermann, and P. Werner, Phys. Rev. B **90**, 195114 (2014).

[54] C. Taranto, S. Andergassen, J. Bauer, K. Held, A. Katanin, W. Metzner, G. Rohringer, and A. Toschi, Phys. Rev. Lett. **112**, 196402 (2014).

[55] A. Toschi, A. A. Katanin, and K. Held, Phys. Rev. B **75**, 045118 (2007).

[56] A. A. Katanin, A. Toschi, and K. Held, Phys. Rev. B **80**, 075104 (2009).

[57] T. Schäfer, F. Geles, D. Rost, G. Rohringer, E. Arrigoni, K. Held, N. Blümer, M. Aichhorn, and A. Toschi, Phys. Rev. B **91**, 125109 (2015).

[58] A. Valli, T. Schäfer, P. Thunström, G. Rohringer, S. Andergassen, G. Sangiovanni, K. Held, and A. Toschi, Phys. Rev. B **91**, 115115 (2015).

[59] A. N. Rubtsov, M. I. Katsnelson, and A. I. Lichtenstein, Phys. Rev. B **77**, 033101 (2008).

[60] A. N. Rubtsov, M. I. Katsnelson, and A. I. Lichtenstein, Ann. Phys. **327**, 1320 (2012).

[61] E. G. C. P. van Loon, A. I. Lichtenstein, M. I. Katsnelson, O. Parcollet, and H. Hafermann, Phys. Rev. B **90**, 235135 (2014).

[62] H. Hafermann, S. Brener, A. N. Rubtsov, M. I. Katsnelson, and A. I. Lichtenstein, J. Phys.: Condens. Matter **21**, 064248 (2009).

[63] A. M. Sengupta and A. Georges, Phys. Rev. B **52**, 10295 (1995).

[64] H. Kajueter, Interpolating perturbation scheme for correlated electron systems, Ph.D. thesis, Rutgers University, 1996 .

[65] Q. Si and J. L. Smith, Phys. Rev. Lett. **77**, 3391 (1996).

[66] See Supplemental Material at http://link.aps.org/supplemental/10.1103/PhysRevB.92.115109 for details on the computation of the vertex, on the estimation of $\overline{T}$ and on the influence of the decoupling choice.

[67] F. Aryasetiawan and S. Biermann, Phys. Rev. Lett. **100**, 116402 (2008).
[68] J. Kuneš, Phys. Rev. B **83**, 085102 (2011).
[69] A. N. Rubtsov, V. V. Savkin, and A. I. Lichtenstein, Phys. Rev. B **72**, 035122 (2005).
[70] P. Werner, A. Comanac, L. de' Medici, M. Troyer, and A. J. Millis, Phys. Rev. Lett. **97**, 076405 (2006).
[71] P. Werner and A. J. Millis, Phys. Rev. Lett. **99**, 146404 (2007).
[72] J. Otsuki, Phys. Rev. B **87**, 125102 (2013).
[73] H. Hafermann, Phys. Rev. B **89**, 235128 (2014).
[74] O. Parcollet, M. Ferrero, T. Ayral, H. Hafermann, P. Seth, and I. S. Krivenko, Comput. Phys. Commun **195**, 401 (2015).
[75] H. Park, K. Haule, and G. Kotliar, Phys. Rev. Lett. **101**, 186403 (2008).
[76] A. Damascelli, Z. Hussain, and Z. Shen, Rev. Mod. Phys. **75**, 473 (2003).
[77] B. Kyung, G. Kotliar, and A.-M. S. Tremblay, Phys. Rev. B **73**, 205106 (2006).